1998ncdb.conf...93C

# The Soil Record of an Exceptional Event at 4000 B.P. in the Middle East

**Marie-Agnès Courty**

*C.N.R.S.-C.R.A., DEMOS, AGER, Institut National Agronomique P-G, F-78850 Grignon, France*

## Summary

Further investigations have lead us to re-examine the nature, age, causes and effects of the third millennium catastrophe that we first identified as an abrupt climate change dated at 2200 BC, synchronous to a volcanic event, and inferred to have initiated the collapse of the Akkad Empire. Comparison of natural soil sequences and third millennium BC archaeological deposits across northern Syria have allowed us to identify the regional trace of this exceptional event that is represented by a thin dust layer showing great spatial variability due to differences of preservation conditions and non- uniform manifestations. Deposition of the dust layer occurred just after a disruption of surface soils, possibly caused by a shock wave well-documented in archaeological sites, with rapid propagation of a wild-fire, and was synchronous with the fall-out of black carbon originating from major forest fires in other regions. The event was immediately followed by exceptional heavy rain storms. Radiometric dating provides an age at ca. 4000 B.P. ( i.e. 4500-4100 cal B.P. at 2 $\sigma$), consistent with the chronological estimation based on archaeological data from reliable contexts: the transition between late Early Dynastic III and Early Akkad (i.e. 2350-2300 cal BC). Its petrographic assemblage indicates ejection of rock fragments from various exogenous geological formations (marine limestone, basalts, gabbros, sandstones) and a great diversity of rounded, well-sorted spherules and vesicular glassy grains deriving from vaporised rocks. Re-interpretation of the previously-found thick tephra-rich deposit allows us to demonstrate that it represents a lateral variation of the dust layer and originated from long distance transport of volcano-sedimentary formations by unusual air turbulence. This exceptional accumulation over 1 km$^2$ area of exogenous deposits is no longer taken to trace a tephra fall-out from a volcanic explosion but confirms that the event is marked by massive ejecta originating from volcanic terrains.

The exceptional manifestations recorded during this event explain our previous confusion with a volcanic explosion and an abrupt climate change. The origin of this mysterious phenomenon still remains unsolved. A better comprehension of the micro-debris fall-out and factors responsible for spatial variability of the signal should help to test further the hypothesis of an explosion caused by disintegration of an extra-terrestrial projectile.

## 1. Introduction

The fallout of a massive tephra layer and the synchronous large increase of wind turbulence observed from various soil contexts of north-eastern Syria were previously interpreted by us [29] as exceptional manifestations linked to an abrupt climate change at around 3.9 kyr B.P., based on stratigraphic correlation with Tell Leilan archaeological sequence (29). The strict contemporaneity between the abandonment of Tell Leilan and the uncommon aridification lead us to propose a causal linkage between a unique deterioration of environmental conditions in northern Syria with a profound destabilisation of socio-economic systems that could have played a crucial role in the collapse of the Akkad Empire domination over northern Mesopotamia.

Synchronous social collapse, as previously documented in Egypt, Indus and the Agean region, and evidence for an aridity peak at 3.9 kyr B.P. from west Africa to west Asia, served to support the global dimension of the climate disturbance and the related socio-economic crisis [11, 16, 28]. Both aspects have, however, remained severely disputed because of the difficulty in obtaining high chronological resolution for relating different strands of evidence in real time and the common hostility towards viewing the trajectory of ancient societies as punctuated by a series of natural catastrophes [4, 12, 13, 30].

Evidence from the Gulf of Oman has recently reinforced the hypothesis of a unique and global scale event marked by the twinned manifestation of "tephra fallout/dust pulse" [28]. It was suggested, however, that long distance correlation should be considered cautiously given the uncertainties of carbon dating [12].

Surprisingly, the dating evidence for less than about 140 years between fallout of the volcanic ash and the dust pulse obtained in the Gulf of Oman [12] has not been used to confute the climate/historical linkage suggested by us in 1993 [29] on the basis of our previous interpretation of late third millennium soils. The search for large-scale connections and a precise quantitative estimate of the aridity increase seems to have concealed important questions regarding the essence of the ca. 3900 B.P. unique event: (1) the significance of a volcanic deposit showing an uncommon spatial variability and its linkage with the dust spike; (2) and the succession in real time of the related manifestations, reasons for their spatial variability and refined correlation with historical events?

Here, we report the progress of our investigation in northern Syrian extended to additional archaeological sites and natural soil sequences that now allow us to establish the existence of the dust layer on a regional scale. The research strategy was adapted to provide the quality of data necessary for debating the exact nature of linkages between natural phenomena and human behaviour on a time-scale compatible with the one for societal phenomena. This paper presents arguments for the detrital origin of the previously-found tephra and for their deposition by exceptional long-distance air turbulence. We speculate on the special circumstances that produced at the same time a massive dust increase generated by pulverisation of the local soils together with an exogenous component, wild-fires and subsequent heavy rains, and envisage a cosmic hypothesis.

## 2. Research strategy

The original results reported here have greatly benefited from detailed soil investigations carried out successively in various parts of the Upper Jezireh [5, 8, 10]. Homogeneity of geological materials, landform monotony due to extensive gentle flooding and dust accretion in addition to a profusion

© Archaeopress • Provided by the NASA Astrophysics Data System

nouvelles.conf...93C

Marie-Agnes Courty

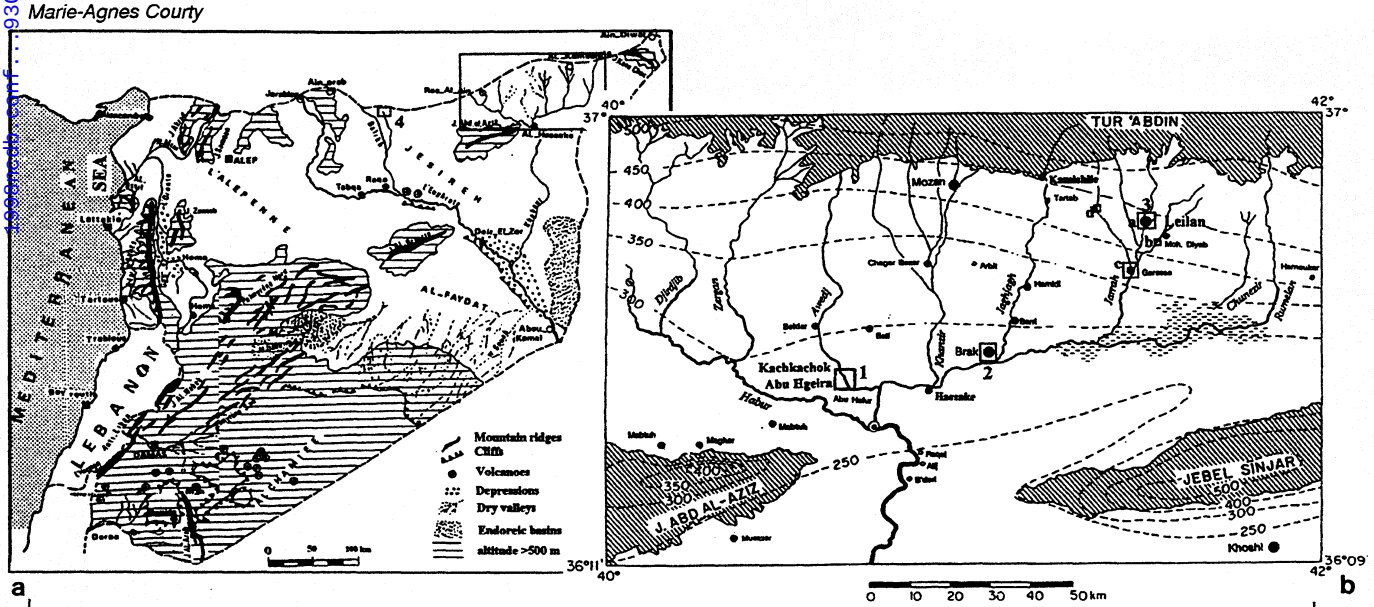


**Fig. 1a**. Location map of the study areas in the Middle East: Northern Jezireh (large rectangle) and Tell Chuera, upper Balikh valley (4). **Fig. 1b**. Location of the studied areas in the Northern Jezireh region: (1) Abu Hgeira 2 and Abu Fur; (2) Tell Brak; (3a) Tell Leilan; (3b) Abu Fara; (3c) Chura; (3d) Tell Aïd.

of well-preserved archaeological sites have provided optimal conditions to trace spatially from the profile level and the micro-region up to the regional level the unique environmental change that occurred at the end of the third millennium BC. An important research effort was devoted to identify ideal situations offering excellent preservation for the soil signal of this unique event and high resolution dating. The best record was obtained from natural soils subsequently buried below archaeological deposits. In addition comparison with soil sequences from active depositional environments has allowed us to obtain a better understanding of the nature and intensity of geomorphic factors that obscure the signature of short-term events. Aware of the inherent difficulties in precisely bracketing abrupt environmental changes by radiometric dating, microstratigraphic studies have been simultaneously performed on archaeological sites to determine the exact chronological position of this exceptional event in occupation sequence, establish its strict contemporaneity between distant sites and, in an improved fashion test the existence of direct linkages between natural phenomena and cultural changes.

We report, here, results from four micro-regions located in north-eastern Syria (Fig. 1) that have been studied at different levels depending upon the practical facilities operating in the field (Table 1).

## 3. Analytical procedure

The progress of investigations has lead us to elaborate a flexible analytical procedure designed to detect, quantify and explain all kinds of diagnostic signatures specific to this unique event. The inventory was achieved through a systematic comparison with soils and sediments formed during the Holocene, their modification under the influence of successive climate changes and their transformation by human activities. Considering the great homogeneity of parent materials and a weak differentiation of soils, the study of soil and sediment properties was performed under the petrographic microscope by comparing 900 large thin sections (13 x 7 cm) prepared from undisturbed samples.

The difficulty in recognising with the naked eye clear manifestations of the event has caused us to adopt a back-and-forth strategy between the field and the laboratory in order to determine its exact stratigraphic position and refine later sampling. Rapid examination in thin sections of the deposit micro-facies has provided the most secure diagnostic by allowing simultaneous study of mode of deposition, petrography of each deposit and its soil microfabrics. Under the petrographic microscope, various millimetre-sized rock fragments and uncommon particles have appeared to be specific to this event, thus offering the possibility of performing a preliminary control in the field by using a portable binocular. Large amounts of specimens obtained by random sampling have, therefore, been collected, immediately processed through water-sieving and observed under the

| N° | Region | Benchmark site | Nature of investigations |
|---|---|---|---|
| 1 | Lower Awedj valley | Abu Hgeira 2, 2nd millennium | micro-regional study: systematic deep trenches; comparison of buried and surface soils |
| 2 | Lower Jagh Jagh valley | Tell Brak, 5th-2nd millennium | study of occupation deposits from the second half of the 3rd millennium |
| 3a | Central Jarrah valley | Tell Leilan, 5th-2nd millennium | (1) extensive study of 3rd millennium occupation deposits; (2) micro-regional study: systematic deep trenches; comparison of buried and surface soils |
| 3b | Central Jarrah valley | Abu Fara, 2nd millennium | micro-regional study: systematic deep trenches; comparison of buried and surface soils |
| 3c | South-central Jarrah valley | Qarassa, 3rd-2nd millennium | micro-regional study: systematic deep trenches (surface soils) |
| 3d | Western Jarrah valley | Tell Aïd, 4th-2nd millennium | micro-regional study: systematic deep trenches; comparison of buried and surface soils |
| 4 | Upper Balikh valley | Tell Chuera, 4th-3rd millennium | study of occupation deposits from the second half of the 3rd millennium |

**Table 1**. Summary of the investigations carried out in the different regions studied (see locations in Fig. 1).

© Archaeopress • Provided by the NASA Astrophysics Data System

1998ncdb.conf...93C



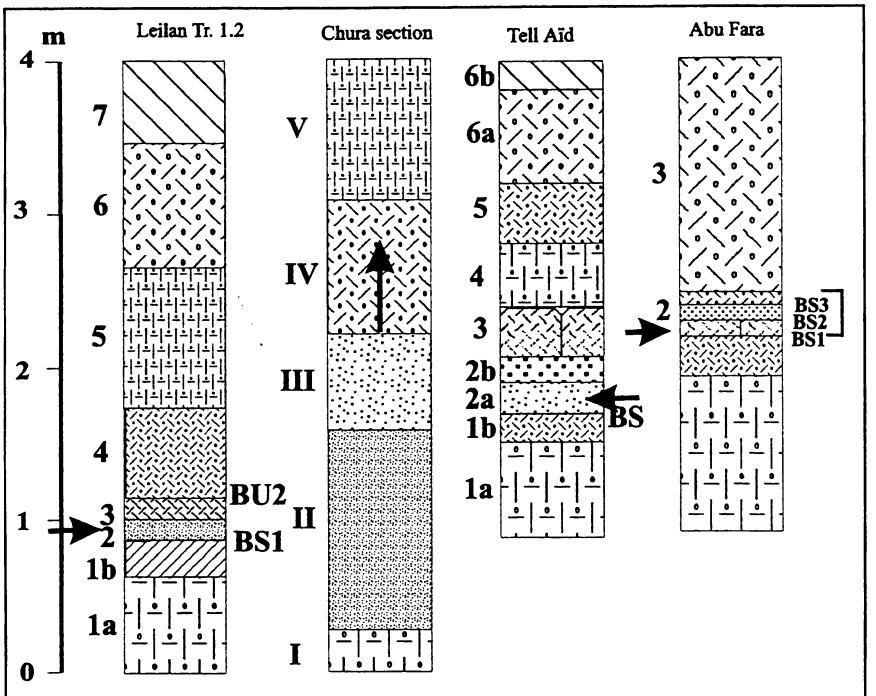


**Fig. 2.** Selection of natural sequences illustrating variability of the stratigraphic position of the thin dust layer in the region of Tell Leilan. Leilan Tr. 1.2 upslope position (3a): (1a) natural soil; (1b) buried burnt upper horizon; (BS1) lower burnt soil surface; (2) the thin dust layer with high spherule content; (3) upper burnt unit, colluvium from 1b, BS1 and 2; (4) single phase mud flow; (5) 2nd millennium B.C. cummulic soil; (6) late Holocene cummulic soil; (7) surface soil. Chura section, active depression (3c): I to IV are stratigraphic units resulting from intermittent flooding and weak pedogenesis; relicts of unusual mineral grains appear at the contact III/IV and throughout IV, with evidence of burning and uncommon calcitic features; (V) last flooded unit, strongly pedogenised. Tell Aïd (3d): (1a) natural soil; (1b) buried burnt upper horizon; (BS) burnt soil surface (2a) micro-layered dust unit with high spherule content; (2b) micro-aggregated coarse unit, colluvium from 1b, BS and 2a; (3) single phase mud flow; (4) cummulic soil; (5) weakly pedogenised slope colluvium; (6a) active soil; (6b) surface horizon. Abu Fara (3b): (1a) natural soil; (1b) buried burnt upper horizon; (2) micro-stratified sequence showing alternation of thin dust layers and burnt surfaces; (3) Second millennium BC. archaeological layers. The arrow indicates the stratigraphic position of the thin dust layer.

binocular. Abundance of the diagnostic particles from the different fractions -sized estimated in the field has allowed us to select the best preserved situations for performing detailed stratigraphic investigations and obtaining high quality samples for various analyses.

Radiometric dating through AMS and conventional methods was restricted to distinct *in situ* burnt ancient surfaces for natural soils and to concentrations of charred remains from thin ashy layers in occupation deposits in order to obtain reliable age estimations. X-ray analysis of the clay fraction (2) and measurement of the black carbon content (soot) was performed from bulk samples collected from the distinct burnt ancient surfaces [6, 23].

100 g to 1 kg of bulk sample was water-sieved using distilled water, applying minimum hand pressure in order to minimise risk of pollution and preserve as far as possible the most fragile particles. Eight fractions were collected: (1) > 2mm, (2) 2-1 mm, (3) 1 mm-500 µm, (4) 500-200 µm; (5) 200 - 100 µm; (6) 100 - 50 µm; (7) 50-25 µm; (8) < 25 µm. An inventory of petrographic assemblages was performed under the binocular for fractions 1 to 6 and under the petrographic microscope for fraction 7. $\delta^{13}C$ and $\delta^{18}O$ isotope measurement was performed on carbonate spherules extracted from

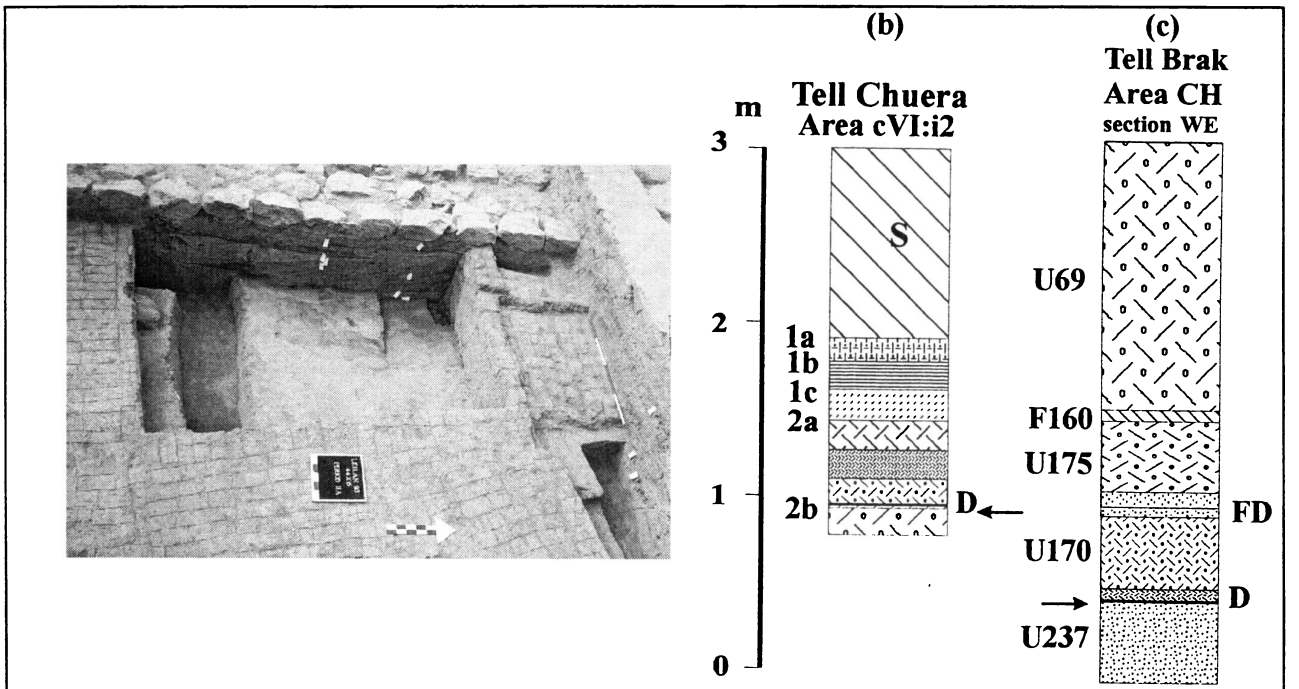


**Fig. 3.** (a) Tell Leilan, 1993 excavation, square 44X15. Stratigraphic position of the thin dust layer (arrow) between the period IIA brick platform and the period IIB (Akkadian levels) basalt architecture. Excavation H. Weiss. (b) Tell Chuera 1997, stratigraphic position of the thin dust layer (D) in square Ci:VI2 at the transition between late early Dynastic III levels (2b) and Akkadian levels (1b); succession of dumped layers and occupation floors. Excavation W. Orthmann and A. Pruss. (c) Tell Brak 1997, stratigraphic sequence from area CH, West-East section, showing an expanded signal of the event in a narrow passage area between mud brick walls; D: first occurrence of the dust with evidence of explosion; FD: fine dust layer; U237: late early Dynastic III levels; U170, U175, F160: transition EDIII/early Akkad; U69: pre-Akkadian floor preparation. Excavation D. and J Oates.



© Archaeopress • Provided by the NASA Astrophysics Data System

1998ncdb.conf...93C


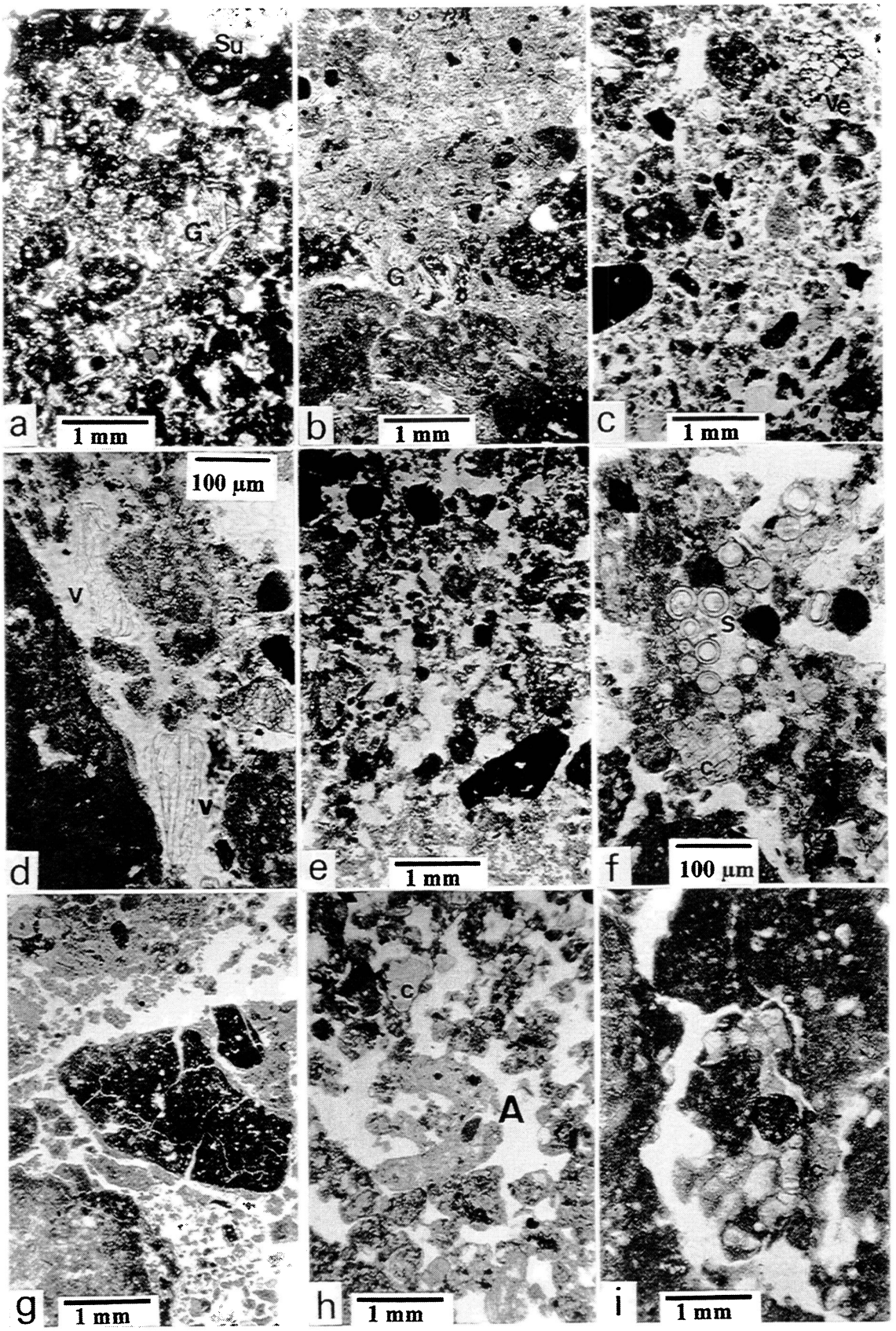


**Fig. 4.** Micro-photographs showing various aspects of the thin dust layer in different contexts. (a) Abu Fur, burnt soil sealed below second millennium occupation deposits, exploded fabric and exogenous particles. (b) Tell Chuera Ci:VI2, level 2b, exploded fabric and exogenous particles. (c) Tell Brak, CH, lower dust layer, exploded fabric and exogenous particles. (d) Enlargement of (c) showing tephra particles. (e) Tell Brak, CH, upper dust layer. (f) Enlargement of (e) showing high concentration of small sized calcite spherules. (g) Leilan Tr. 1.2, burnt soil surface showing an exploded fabric. (h) Section north of Tell Leilan, exploded structure with elongated glass-rich aggregate (A). (i) Chura section, bottom level IV, relict features of the thin dust layer: concentration of exogenous particles and fine crack filling by fibro-radiated calcite.


© Archaeopress • Provided by the NASA Astrophysics Data System

1998ncdb.conf...93C



fractions 5 and 6 of the layer showing the highest concentration of these specific particles.

X-ray analysis was performed on the total residue for fractions 7 and 8 by using a conventional detector and from individual grains for fraction 4 to 6 by using a linear detector. Uncommon grains sorted under the binocular were studied under SEM equipped with EDS microprobe on clods (secondary electrons) and from polished thin sections (back-scattering).

## 4. Stratigraphic variability

Further field investigations performed simultaneously on natural soils and archaeological sites have allowed us to extensively trace over the studied region the thin dust layer (Fig. 2 & 3) first identified as a 0.5 cm-thick unit in the late Akkadian period IIb stratum at Tell Leilan (cf. Phase 1 in Weiss et al., 1993). In spite of a major research effort we have, however, been unable to detect more traces of the 60 cm thick tephra deposit originally found at Abu Hgeira 2, and correlated with a major volcanic eruption [29]. On the contrary, re-examination of the stratigraphic sequence from Abu Hafur 2, located 2 km farther south from Abu Hgeira 2, has lead us to conclude that the aeolian unit formerly correlated to the thick tephra deposit [29] presents, in fact, the facies and petrographic characteristics of the thin dust layer (Fig. 4a). The latter contains high amounts of unusual mineral grains with a petrographic assemblage broadly similar to the ones of the tephra-rich layer, although the different mineral species occur in different proportions with a great variability not only between sites but also over short distances. The most striking difference lies in the abundance of well-sorted spherules, predominantly made of fibro-radiated calcite spherules (Fig. 5a), whereas sand-sized tephra grains are exceptional (Fig. 4d). Occurrence of these particles is associated with unique manifestations that are not always clear in the field, however unquestionable they may be in thin sections.

The thin dust layer displays in the field rapid spatial variations of the micro-stratigraphy that appears to be best preserved in upslope micro-undulations, but is often gradually obscured along gentle slopes and can even totally vanish in large, low lying depressions. The most complete micro-stratigraphy, as observed at Abu Habur 2 (Fig.1b) and at several study sites of Tell Leilan region (Fig. 1b & 2), shows a one centimetre thick, greyish yellow, loose dust layer directly over a distinct burnt soil surface marked by a millimetric ashy grey layer rich in partially-melted *graminae* phytoliths and carbonised lignified residues. Below the calcinated vegetation layer, a dense network of charred threads forms the relics of the original *graminae* root mat, fossilised by rapid carbonisation and preserved from subsequent disturbances. The original micro-aggregated structure of the surface soil horizon, produced by intense bioturbation, displays an uncommon juxtaposition of angular large aggregates with sharp fissures and loosely packed fine aggregates derived from fragmentation of the former (Fig. 4g).

The burnt soil surface and the associated dust layer are overlaid by a massive and homogeneous soil unit (see Fig. 2) that contains fragments of slaking crusts, and abundant fine charred residues. The uncommon sharpness of the contact with this upper unit as compared to the usual regional soil stratigraphy shows rapid deposition by a mud flow that allowed the burnt soil and the associated dust layer to be instantaneously sealed.

An attempt to trace the diagnostic stratigraphic layer along trenches has shown a rapid and important spatial variability due to partial reworking or complete erosion during the subsequent episode of mud flow (Fig. 2). Therefore, the exact stratigraphic position of the event in sequences from depositional environments that have remained continuously active during the Holocene period, such as active flood plain, cannot be identified in the field but only by detecting petrographic markers of the dust layer under the petrographic microscope.

The large extension of the burnt soil that can be traced at local to micro-regional scales across all types of depositional environments, and recognised from different regions on the basis of stratigraphic correlation, allows us to avoid possible confusion with human related fires. Its close association with the unusual dust layer and the subsequent mud -flow furthermore corroborates the exceptional nature of this event.

Complementary information is provided by archaeological sites where lack of a vegetation cover and juxtaposition of

| Site | Lab. n° | Date (years B.P. ± 1 σ) | cal B.P (range at ± 2 σ) |
|---|---|---|---|
| Tell Brak CH97.1 | Beta-110930, AMS | 4040 ± 50 BP | 4555-4350 BP |
| Tell Chuera CVI:2a-110 | Lyon-473 (OxA), AMS | 3980 ± 55 BP | 4560-4267 BP |
| Tell Leilan Tr 1.2 lower burnt soil | GifA 96233, AMS | 3790 ± 90 BP | 4419-3874 BP |
| Tell Leilan Tr 1.2 upper burnt soil | GifA 96236, AMS | 3980 ± 70 BP | 4782-4180 BP |

**Table 2.** Radiocarbon dates. Beta, Beta Analytic, Miami, Florida; Lyon, Centre de datation par le radiocarbone, Lyon, France and Oxford Laboratory, Oxford, England; Gif, Laboratoire des Sciences du Climat et de l'Environnement CNRS-CEA, Gif-sur-Yvette, France. Calibration was with RADIOCARBON CALIBRATION PROGRAM REV. 3.0.3 by the University of Washington.

areas showing contrasted configuration have offered original conditions to record the event as compared to natural soils. The event is traced by presence over a wide region (Fig. 1b and Fig. 3) of unusual mineral grains that are strictly identical to the ones of the dust layer associated with the burnt soil surface in natural soils. In open-air and unroofed areas (Fig. 3a), the mineral grains are concentrated in a centimetre-thick layer and embedded in a loose grey ashy fine mass. The absence of similar particles in the underlying formations helps to identify the exact stratigraphic position of the dust layer. The upper limit is, often, not so clear because the mineral grains have been finely incorporated in the local materials that have subsequently been re-used for constructions (Fig. 3b). Evidence of trampling and re-flooring after the dust accumulation indicates that human activities were not interrupted by the event. Comparison of the associated ashy layer from the different sites did not allow us to identify specific micro-fabrics that would have facilitated a discrimination between micro-stratified ashy layers common to archaeological sites [7].

Narrow open areas that were initially used as passages

| Site | Tell Brak | Tell Leilan | Tell Chuera |
|---|---|---|---|
| Archaeological period | late EDIII-transition EDIII/early Akkad | late Leilan IIa-transition Leilan IIa/Leilan IIb | late EDIII-transition EDIII/early Akkad |
| Chronological range (years ± 1 σ) | 4240 ± 100/ 3680 ± 100 BP | 4020 ± 65 / 3905 ± 65 BP. (from Weiss et al., 1993) | 2300 BC. ca. 4250 cal. BP. |

**Table 3.** Age estimation of the dust layer based on archaeological data.



© Archaeopress • Provided by the NASA Astrophysics Data System

1998ncdb.conf...93C



between mud-brick constructions, however, display a distinct succession of micro-facies that cannot be confused with anthropogenic ones (cf. Fig. 3c and 4b & 4c). The first occurrence of unusual mineral grains is associated with a structureless micro-facies made of loosely-packed sub-rounded to subangular aggregates, mixed with fine ashes and carbonised plant residues. Lack of compaction indicates instantaneous desegregation that strongly contrasts with the progressive accumulation generally found in passage areas [3]. Another uncommon feature is the joint occurrence of aggregates arising from fragmentation of the adjacent constructions and biogenic aggregates that are only present in the surface horizons of the surrounding natural soils. Exceptional elongated aggregates made of densely packed flaky, acicular calcite crystals embedded in a yellow isotropic glassy matrix are also observed (Fig. 4h). The sequence, then, shows a decrease of the ash component and ends with a ca. 2 cm thick dense, structureless, yellowish grey layer made of densely packed silt-sized aggregates with a few coarser particles similar to the unusual mineral grains of the lower dust layer (Fig. 4e). This layer contains high amounts of well-sorted spherules, predominantly made of the fibro-radiated calcite type, that are petrographically identical to the ones often found in the dust layer and in the tephra-rich accumulation, although of smaller size (Fig. 4f). The fine textured dust layer is sealed by various occupation deposits, such as well-prepared floors and dumped materials intentionally laid down for preparing a new phase of construction. Therefore, it represents the last unusual manifestation of the event that clearly occurred during a phase of continuous occupation.

## 5. Chronology of the event

The synchronous occurrence of the various manifestations recorded both in natural landscapes and archaeological sites is fully confirmed by the convergent series of $C^{14}$ radiometric dating (Table 2). Besides aspects related to variability of $C^{14}$ activity during this time period, the reverse order of radiometric ages as compared to the stratigraphic succession of the two burnt layers in the natural sequence close to Tell Leilan (Table 1) warns of the difficulty of using measurement of $C^{14}$ activity for defining the exact age of the event.

Comparison between the three cultural sequences reported also shows a consistent chronostratigraphic position of the event that correlates with the EDIII/Akkad transition both at Tell Brak [18] and Tell Chuera (19), equivalent to the Leilan IIa/Leilan IIb transition at Tell Leilan [27], (Table 3). For the three sites studied, and more particularly for Tell Leilan in which we have performed since 1993 systematic investigations on the third millennium occupation sequences, the series of floors and/or construction deposits that separate the first occurrence of the dust layer *in situ* and the mature Akkad phase provides a secure record to position the event a few decades before the Akkad period, i.e. at ca. 2300-2350 BC on the basis of historical sources [19]. The dust layer has, thus, been easily traced over a 600 $m^2$ area opened during the 1993 season: exactly located just above the Leilan IIa brick platform and well-sealed below huge basalt blocks brought to the site during Leilan IIb phase, i.e. Akkad period (Fig. 3a). This highly-secured stratigraphic context allows us to re-adjust the exact age of the event to be 150 years older than the first age estimation (2200 BC) as given in Weiss et al., 1993.

## 6. Evidence for regional wild fires

A significant increase of the black carbon content that exactly coincides with the distinct burnt soil surface associated with the dust layer was measured at three localities in the region of Tell Leilan (Fig. 5). Intensity of the black carbon increase is typical of a high temperature fire that produced high amount of smoke, such as the ones related to burning of a dense savannah or tropical forest [6]. This increase cannot be explained by combustion of the local biomass which at that time consisted of a graminae cover in cultivated fields, an open shrubby steppe in non-cultivated areas and gallery forest along river channels. Rapid decrease of the black carbon content in later soil horizons, however rich in charred plant remains (Fig. 5a), or in occupation layers with high amounts of fine charred residues (Fig. 5c), confirms that endemic local fires, either natural or human-related, do not produce significant black carbon increases. Moreover, absence of detectable clay alteration in the topmost part of the burnt soil surface proves that combustion of the local vegetation occurred instantaneously and that the soil heating has remained surficial [2]. These contradictory facts can be reconciled by relating the black carbon increase to an exogenous input that would have arrived, together with the mineral grains, via air transport from major biomass-

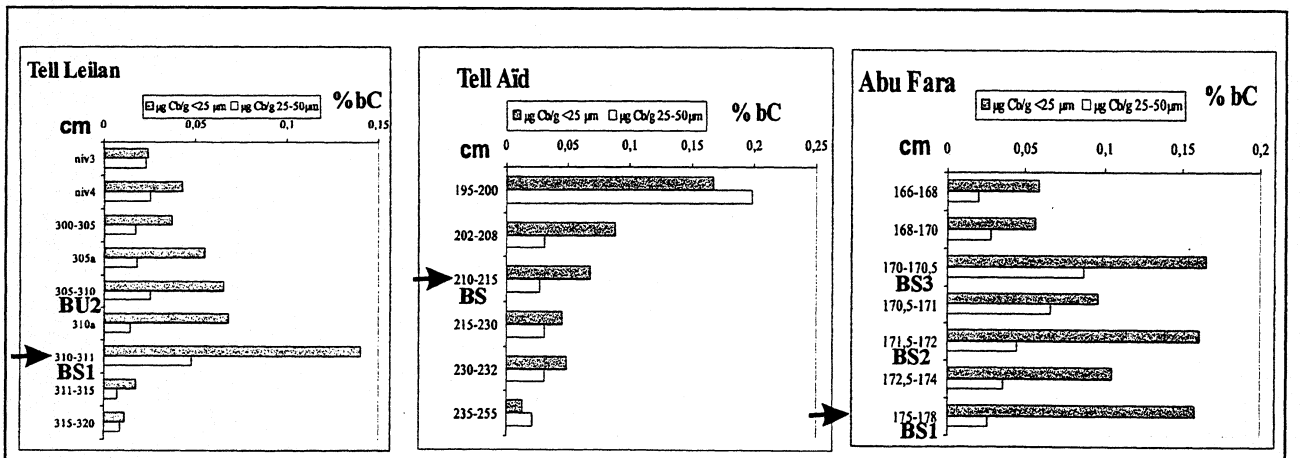


**Fig. 5.** Measurement of black carbon content (a) Tell Leilan tr. 1.2: marked increase at the exact stratigraphic position of the dust layer; (b) Tell Aïd: marked increase just above the burnt soil surface; (c) Abu Fara: high content in the three burnt surfaces associated with the thin dust layer, decrease in the upper ashy archaeological deposits (cf. section in Fig. 2).

© Archaeopress • Provided by the NASA Astrophysics Data System

1998ncdb.conf...93C



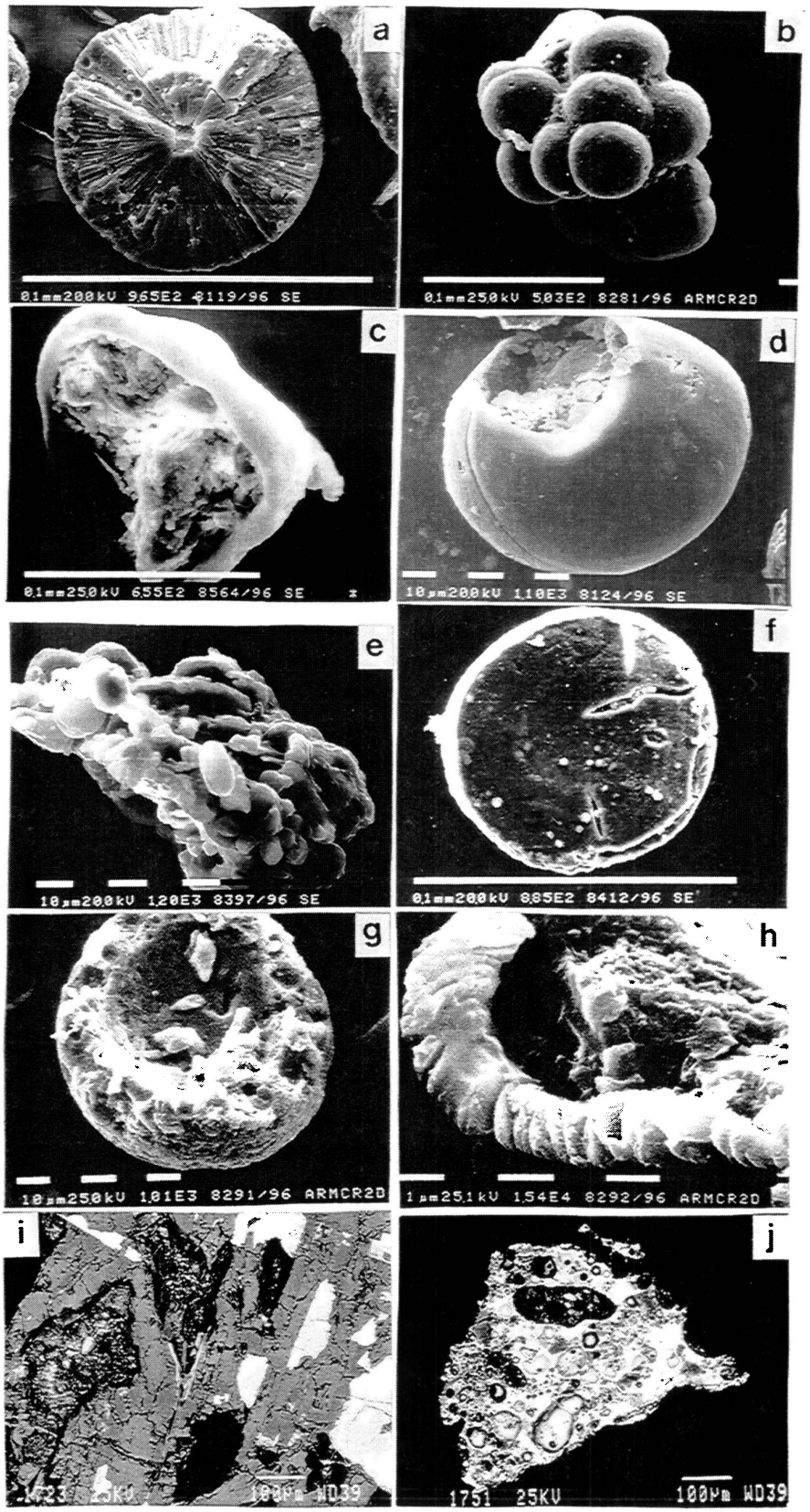


**Fig. 6.** SEM views of the thin dust layer at Tell Leilan Tr. 1.2. (a) single fibro-radiated calcite spherule, sectioned when air transported and (b) multispherules strongly bound together by silicate cements; (c) translucent, dull orange, tailed-shape, ankerite spherule; (d) silica spherule with Mg carbonate fill; (e) KCl white aggregate; (f) phosphate spherule with KCl small spherules; (g) alumino-silicate spherule; (h) enlargement of (g) showing the ribbon-shape tail made of nickel-rich tiles; (i) angular gabbro fragment with potassium rich glass as infilling of the feldspar fine cracks; (j) complex vesicular glass particle that contains metallic nickel inclusions.



© Archaeopress • Provided by the NASA Astrophysics Data System

1998ncdb.conf...93C



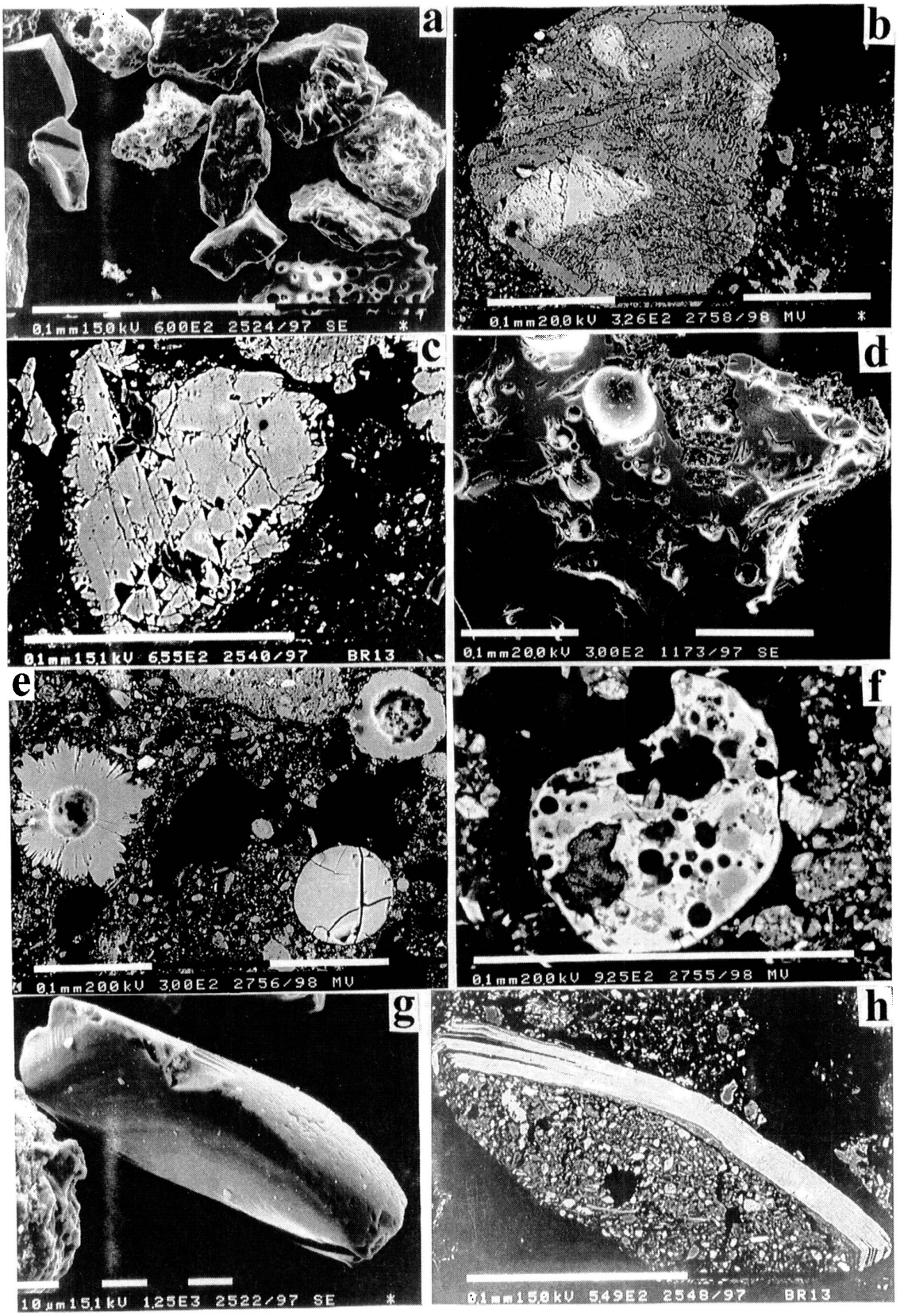


**Fig. 7.** Petrographic composition of the thin dust layer at Tell Brak.(a) Angular coarse silt (50-25 µm): quartz (1), feldspar (2), vesicular silica grain (3); (b) various highly fissured angular quatzitic sandstone; (c) carbonate fragment showing an uncommon dissolution produced by $CO_2$ degassing; dark zones correspond to local replacement of carbonates by silica ; (d) carbon-rich (~50%) angular, black, vesicular grain with vesicle infilling made of Mg-Ca rich alumino-silicate glass and pure silica glass; (e) to (f) Specific aspects of the fine-textured dust layer: (e) 50-100 µm spherules, fibro-radiated calcite (1), phosphate (2), silica/carbonate (3); (g) diatom with a pitted weathered surface; (h) elongated fibrous amphibole embedded in fine dust made of acicular crystals.



© Archaeopress • Provided by the NASA Astrophysics Data System

1998ncdb.conf...93C



burning in forested regions [14].

A significant black carbon increase of similar intensity as the one found in natural soils was also measured from occupation deposits of Tell Leilan at a stratigraphic position that exactly coincides with the thin dust layer, well-defined by the sharp increase of exogenous grains [1].

## 7. Petrography of the thin dust layer

The great variability of the micro-debris assemblages observed between distant sites and at short distance concerns the relative amount, particle-size distribution and properties of the different types of coarse particles identified: spherules, glass particles, fragments of igneous rocks, exogenous carbonates, salts and micro-fossils.

The most comprehensive characterisation of the spherule component was achieved on the dust layer traced over Tell Leilan region (Fig. 1) in which the spherule proportion locally reached 50% of the total dust mass. They are well sorted with an average size between 100-50 µm and a minor proportion in the fraction 200-100 µm. Five mineralogical types have been recognised: carbonate spherules are largely dominant, mainly formed of calcite (Fig. 6a, 6b, 6c & 7e) and in a minor proportion of Mg-rich carbonates (Fig. 7e), amorphous phosphate (Fig. 6f & 7e), silicates (Fig. 6d), alumino-silicates (Fig. 6g), spherules of iron oxides and chromites.

Pure calcite spherules present a granular or a smooth surface and are either white, grey , black, or bi-coloured (internal white part with an external black part, or the reverse); single spherules are predominant (Fig. 6a) and occur together with a minor proportion of multispherules strongly bound together by silicate cements (Fig. 6b). The proportion of major elements is identical for spherules of different colour. KCl is often present as micron-sized crystals or small spherules included in the silicate cement or bound to the surface of the calcite spherules (Fig. 6f). The calcite spherules always display a radiating pattern of densely crystallised needles that show epitaxic growth features and a crystalline continuity from the centre to the outer part (Fig. 6a). Common presence on the sectioned face of the broken spherules of small craters juxtaposed to small calcite spherules of exactly the same size that resisted water-sieving (Fig. 6a) shows that fragmentation, surface transformation caused by ejection and trapping of carbonate droplets occurred during the process of spherule crystallisation and were not caused by laboratory treatment.

Calcite spherules rich in Mg are yellow, generally present an irregular mammilated surface and can display either a continuous fibrous-radiated crystalline fabric or a concentric one. They occur together with spherules of dolomite and ankerite rich in Si that are translucent, dull orange, tailed-shape, showing a smoothened outer part and a finely crystallised inner part (Fig. 6c). The major element composition of the inner and outer part are broadly similar except for the presence of chlorine (~ 1%) in the outer part and in the twisted tail. These orange spherules are extremely fragile and often break during laboratory treatment, losing the twisted tail which can be originally more than 200 µm long. A specific type of orange spherule with the twisted tail, but empty, was observed under the binocular but was severely damaged during careful sampling. The carbonate spherules

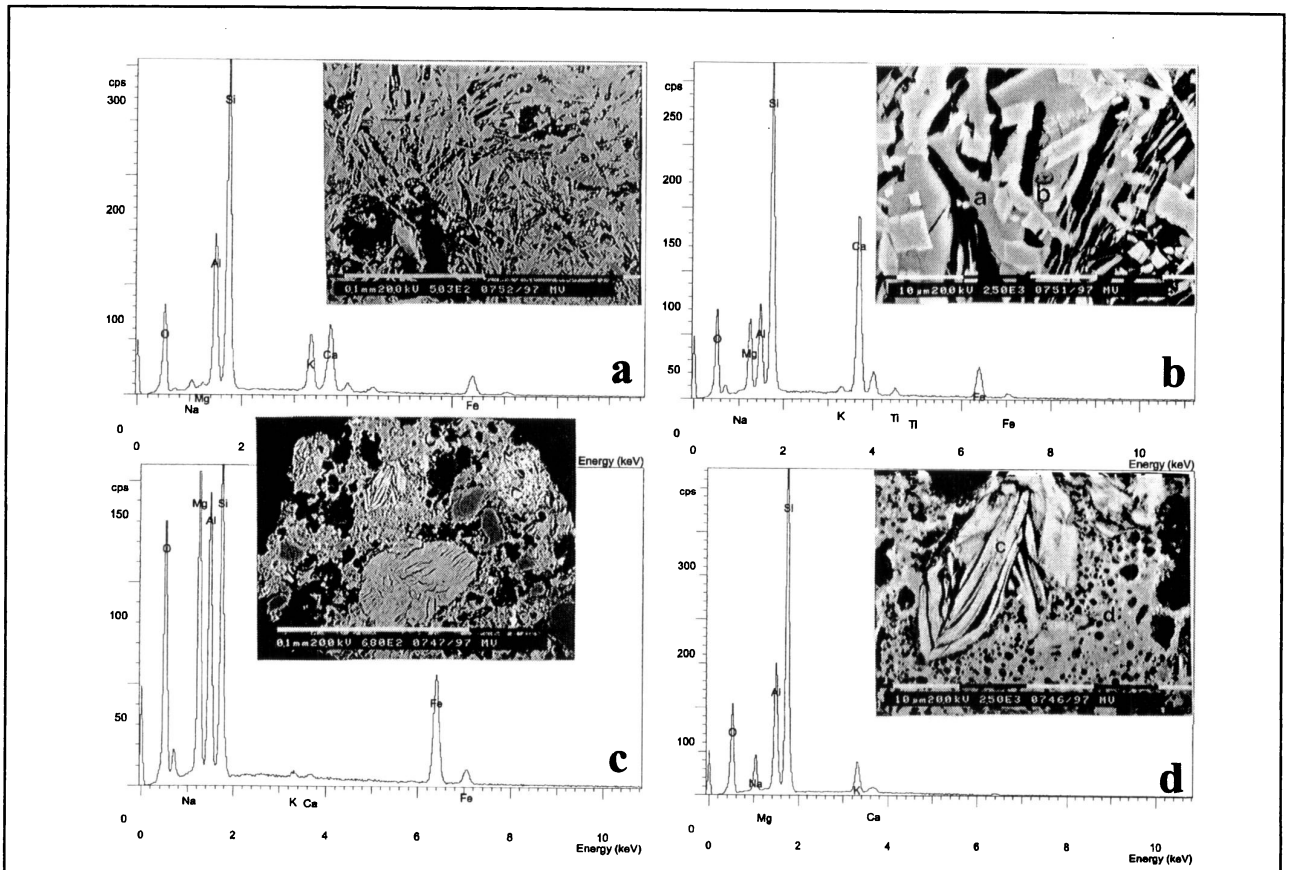


**Fig. 8.** SEM views and EDS analysis of unusual grains of the thin dust layer at Tell Chuera. (a) Greyish yellow vesicular grain made of needle-shape pyroxene crystals; (b) detailed view of (a) showing the micron-sized acicular pyroxene crystals floating in glass; (c) greyish yellow vesicular grain showing relicts of sands (quartz, amphibole, K-feldspar, argilite) embedded in a K-rich glass; EDS analysis: composition of the fibrous amphibole; (d) detailed view of the grain in (c) and the glassy matrix; EDS analysis: composition of the potassic glassy matrix.



© Archaeopress • Provided by the NASA Astrophysics Data System

1998ncdb.conf...93C



present the following isotopic composition:

$\delta^{13}C$ = -14.7 +/- 0.2 ‰ (PDB)

$\delta^{18}O$ = 23.3 +/- 0.2 ‰ (SMOW).

Pure silica spherules are generally translucent to white, well-rounded, with a smooth surface. In polished section they display a concentric fabric or are undifferentiated, with empty vesicles of various sizes. Some silica translucent spherules are empty with an external silica collar, very fragile and easily broken during sampling. Similar white spherules with a concentric fabric display a compound composition of silicates and carbonates (Fig. 6d & 7e). Spherules of alumino-silicates are generally smaller (80-30 µm), yellowish brown to dark brown, formed of densely-packed needle-shaped crystals of pyroxene, with a great variability of their major element composition, that are embedded in a porous calco-potassic glass (Fig. 6g). Exceptionally, these alumino-silicate spherules present on their external part a ribbon-shape tail made of densely packed nickel-rich tiles (Fig. 6h) that are coated and cemented by alumino-silicates of similar composition to the host spherules, except for the presence of chlorine in traces (~ 1%).

Phosphate spherules are generally pale yellow to yellowish brown, smooth, undifferentiated, finely fissured and often present as micron-sized spherules of KCl strongly attached to the surface (Fig. 6f).

The presence of KCl has also been identified in the form of white grains made of densely packed and strongly cemented ovoid particles made only of this highly soluble salt (Fig. 6e).

The spherules and associated particles are embedded in a pale yellowish brown fine mass formed of very fine silt-sized carbonate particles mixed with clay and with abundant quartzitic, silt-sized, grains. Although apparently similar to the ones of the surrounding soils, various subtle differences suggest that a large part of this fine mass is not of local origin: the abundance of dolomite grains that are never present in the local soils; the angular shape of the quartz and feldspar grains (Fig. 7a) generally coated by reddish brown clay; the abundance of vesicular silica grains; and the common presence of fresh muscovite, biotite and fibrous amphibole and bassanite in the form of silt-sized crystals.

An important component of the micro-debris layer is represented by fragments derived from igneous rocks that range from a few millimetre-sized polycrystalline grains to smaller individual phenocrysts of pyroxene, olivine or Ca-feldspar. The great proportion of coarse crystallised igneous rocks of gabbro type made of large, unweathered olivine, plagioclase and pyroxene (Fig. 6i) contrasts with the local volcanic rocks (20). The latter consists of vesicular basalts with strongly ferruginised olivine embedded in a groundmass of finely-crystallised feldspars and a low amount of finely crystallised pyroxene. In addition to this petrographic difference, the igneous rock fragments of the dust layer differ from the basalt fragments of the local soils by their angular shape and fresh faces, and also by presence of a potassium-rich glass present as infilling of fine cracks and vesicules of the feldspars. Moreover, they occur together with unusual, millimetre-sized to a few hundred microns, pale yellow to yellowish grey vesicular grains that are either made entirely of undifferentiated glass (Fig. 6j) or are formed of a gabbro core embedded in glass or consisting of micron-sized acicular pyroxene crystals floating in glass (Fig. 8 a & b).

The geochemical composition of the glass is generally not uniform within a grain and greatly varies between vesicular grains of the same dust layer and also between the different sites studied. Two types of glass are commonly juxtaposed: (1) a Ca-Mg rich alumino-silicate glass with variable proportions of Fe and the presence of uncommon inclusions such as pure nickel grains (Fig. 6j), zinc or copper, that can be geochemically defined as a pyroxene glass; and (2) a potassium-rich alumino-silicate glass, generally less dense and devoid of metal-rich inclusions, that is geochemically similar to the one present within the vesicles of the gabbro grains (Fig. 6i) and in the vesicular grains with pyroxene needles (Fig. 8a). The latter K-rich glass also forms the fine matrix of other vesicular grains that contain various sand-sized inclusions (quartz, amphibole, K-feldspar, argilite) and appears to be highly transformed sandstones (Fig. 8c & 8d).

Unusual fragments of various sandstones are also present, generally characterised by highly fissured angular grains (Fig. 7b).

Carbonate grains, either limestone fragments or bioclasts, often display an uncommon weathering pattern resulting from dissolution along cleavage planes that might be produced by $CO_2$ degassing, also associated with the local replacement of carbonates by silica (Fig. 7c).

A common component of the dust layer for all the sites reported here consists of unusual angular, black, vesicular grains that are made predominantly of carbon (~50%) although they do not morphologically resemble either carbonised plant residues or fossil combustibles (Fig. 7d). They are finely fissured, dense and often contain phosphate inclusions. Their large vesicles are often filled by a Mg-Ca rich alumino-silicate glass similar to the type 1 glass described above and a fine vesicular pure silica glass.

The fine-textured dust layer recognised as the last episode of the event at specific localities showing an expanded signal presents a similar petrographic assemblage to the one of the initial dust layer, differing only by the smaller size of the particles and their higher abundance (Fig. 10e & 10f). This greater proportion has allowed a better characterisation of diatoms that were identified in thin sections, occurring either as individual grains embedded in the dust or as aggregates cemented by calcite. In addition to their uncommon presence, SEM observations have revealed a pitted weathered surface and the impossibility of identifying surface features diagnostic of the species (Fig. 10g). Moreover, the very fine dust appears to have been transported as sand-sized complex grains that have suffered minimal fragmentation. This is indicated by the good preservation of fragile fibrous grains (Fig. 10h).

The comprehensive inventory of the dust layer petrography as provided by contexts offering a well-preserved signal has allowed us to identify relict traces of the event in depositional environments that were severely reworked by the subsequent mud-flow as well as from an active flood plain. They comprise rare millimetric fragments of igneous rocks, a marked increase in the coarse silt-sized fraction of individual mineral species derived from the former (pyroxene, olivine, feldspars), occasionally slightly altered calcitic spherules and the presence of uncommon calcitic features along cracks that might derive from pedogenic transformations of the spherule-rich dust layer (Fig. 5i).

## 8. Petrographic re-examination of the thick tephra facies

The 50 cm thick tephra-rich layer found in the buried soil of Abu Hgeira 2 (Fig.1) was originally interpreted as an accumulation derived from a volcanic plume after long-distance transport that would possibly originate from volcanic centres of the Anatolian-Caucasian area [29]. A series

© Archaeopress • Provided by the NASA Astrophysics Data System

1998ncdb.conf...93C



of anomalies not compatible with the volcanic hypothesis has led us to re-examine this interpretation: 1) the restricted distribution of this deposit in spite of its notable thickness; 2) lateral transition between the tephra-rich deposit and the thin dust layer; 3) the failure to confirm the presence of similar tephra grains in the thin dust layer; and 4) the facies

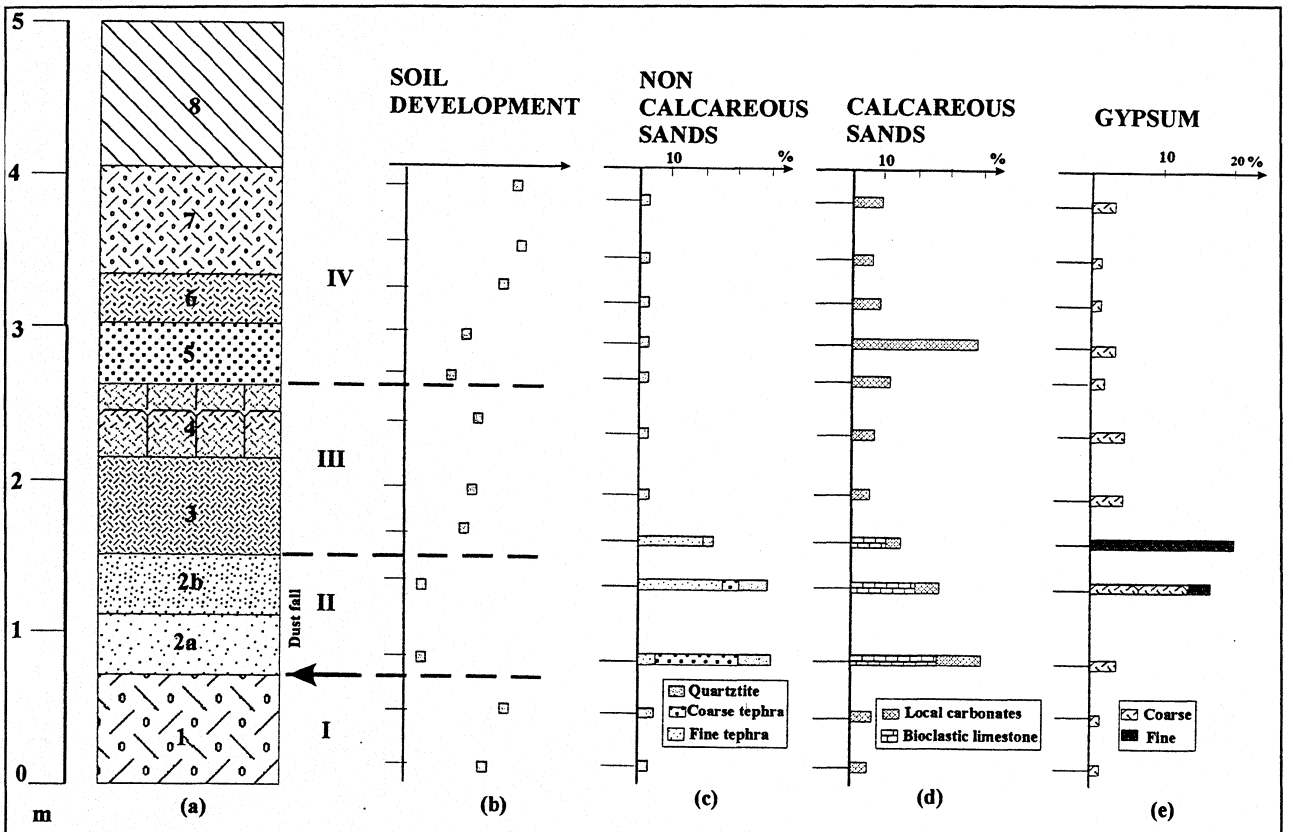


**Fig. 9**. Abu Hgeira 2- (a) Stratigraphic sequence: (1) 3rd millennium BC. soil; (2a) coarse textured tephra-rich deposit; (2b) fine textured tephra-rich deposit; (3) single phase mud flow; (4) weakly pedogenised wind/water layer; (5) coarse-textured colluvium; (6) weakly pedogenised wind/water layer; (7) well-developed buried soil; (8) 2nd millennium BC. occupation deposits; (b) Profile of the soil development index: (Biological activity + Calcitic features/ Sedimentary features); (c),(d), (e) Profile of non-calcareous sands, calcareous sands and gypsum abundance quantified from thin sections.

and petrography of the tephra-rich layer, which are uncommon for a supposed passive fall-out.

A refined examination of the trenches dug across the Awedj flood plain [5] has failed to detect the presence of tephra. Evidence for their progressive weathering along the restoration of a stable soil cover as observed at Abu Hgeira 2 sequence from layers 4 to 7 (Fig. 9) shows that pedogenic weathering is unlikely to have been responsible for their total disappearance as we originally supposed (29). Recognition of the thin dust layer at Abu Hafur 2 (Fig. 4a), located 2 km farther south, now allows us to establish that the thin dust layer represents a spatial variation of the tephra-rich deposit. The latter is, thus, concluded to have accumulated over a restricted area, not exceeding a few $km^2$, possibly favoured by the existence of a small basin at this specific location.

A better comprehension of the tephra-rich layer characteristics reinforces this stratigraphic correlation. Further interpretation concerns, firstly, the pseudo-sand micro-facies at the very bottom of the tephra-rich layer (2a, Fig. 9), just above the third millennium BC. Calcisol, which we originally interpreted as evidence of saltation aeolian transport [29]. The puzzling feature was the abundance of uncommon, millimetre-sized sub-rounded aggregates associated to the 50% sand-sized tephra particles embedded in calcitic silt (Fig. 10b). None of these aggregates resemble the ones normally found in the colluviated soils or the wind-blown deposits common in the studied region [5]. A first type of aggregate (type 1) is characterised by a lenticular microfabric typical of freezing that is totally unusual for the studied region (Fig. 10a). It contains tephra gains in the same proportion and size range as the surrounding matrix. A second type of aggregate (type 2) displays an irregular laminated facies similar to the one of slaking crusts created by heavy rain spells (Fig. 10c) as originally interpreted [29]. However, its petrographic composition, made of fine silt-sized tephra particles, polished diatoms with a pitted surface, and quartz embedded in calcitic silt clearly differs from that of the surrounding soil matrix (Fig. 10d). Less common aggregates show a high concentration of siliceous sponge spicules (type 3, Fig. 10e) whereas others display strong ferruginisation and moderate weathering of the tephra particles (type 4) that contrasts with the fresh aspect of the tephra from the juxtaposed materials (Fig. 10f). The close imbrication of these various aggregates within the loose matrix, their morphology and their good sorting indicate that both components have been deposited together after air transport. Preservation of the frost-induced microfabric for type 1 aggregates suggests that they have been transported as frozen materials. The mineralogical composition of type 2 aggregates rules out a formation *in situ*, following deposition of the tephra-rich layer. They are more likely to be relicts of a sedimentary facies initially present in the formation that supplied the tephra particles and associated components. Composition of type 3 aggregates, totally uncommon for the region, also supports this interpretation. Furthermore, the close juxtaposition of tephra particles at different weathering stages achieved under subaerial conditions (cf. type 4

© Archaeopress • Provided by the NASA Astrophysics Data System

1998ncdb.conf...93C



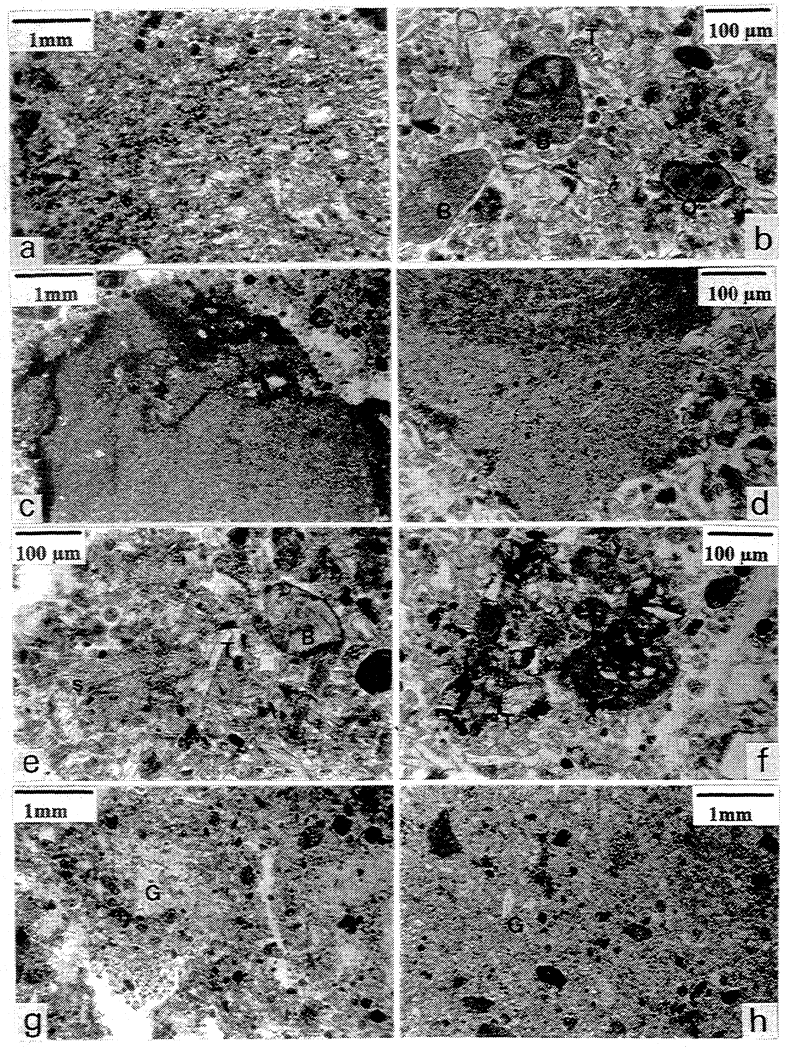


**Fig. 10**. Micro-photographs showing specific aspects of the tephra-rich deposit, Abu Hgeira 2. (a) type 1: tephra-rich aggregate with lenticular microfabric typical of freezing grains; (b) bioclasts and tephra sand-sized grains embedded in calcitic silt ; (c) type 2: surface-crust like aggregate; (d) higher magnification of (c) showing its composition made of fine silt-sized tephra particles and diatoms in calcitic silt; (e) type 3: aggregate with high concentration of siliceous sponge spicules; (f) type 4: ferruginised aggregate with weathered tephra particles; (g) detrital and partly recrystallised coarse gypsum in layer 2a; (h) detrital fine textured gypsum in layer 2b.

aggregates) proves that the tephra component cannot derive from a freshly exploded volcanic plume as we originally concluded [29].

Our previous study focussed on the geochemistry of the tephra particles [29]. Further investigation of the petrographic composition of the non-tephra component and refined examination of the glass geochemistry brings complementary information on the original deposit and transformation that occurred just before its transportation. The petrographic composition of the tephra-rich layer (2a, Fig. 9) shows that a great diversity of exogenous particles has been simultaneously transported and deposited with the sand-sized tephra particles: mainly sand-sized grains derived from bioclastic and dolomitic marine limestone (Fig. 10b and Fig. 11f); in a minor proportion, sand-sized grains originating from a large variety of volcanic, igneous and metamorphic rocks (granite, green schists, amphibolite, metabasalts, gabbro, peridotite), salts, particularly calcium sulphate (gypsum), barium and strontium sulfate (Fig. 9 & 11h); and fibro-radiated calcite spherules generally present as fragments (Fig. 11c). Outcrops of bioclastic marine limestone are not present locally and the amount of this type of rock fragment never exceeds 1% in parent materials of the local soils derived from the alluvial fans formed by repeated erosion of the Taurus foothills [5].

Similarly, local soils and sediments do not contain fragments of dolomitic limestone, characterised by a high magnesium content, or fibro-radiated calcite spherules and both are, thus, concluded to be of exogenous origin. The petrographic diversity of the aluminosilicate sand-sized fraction strongly contrasts with the normal petrographic assemblage of the local sediments that is dominantly formed of quartzitic grains and finely crystallised basalts identical to the local lava flows. Gypsum occurs at the bottom of the tephra-rich layer (2a) as individual euhedral crystals or aggregates of euhedral crystals (Fig. 10g), clearly different from the pedogenic gypsum that is often present in the local soils as channel infilling produced by the capillary rise of sulphate-rich perched ground water. The sedimentary origin of the gypsum is confirmed by the rounded contours of the crystals as seen under SEM which is typical of wind abrasion (Fig. 11g). Evolution towards angular fine sand-sized crystals in layer 2b (Fig. 9 & & 10h) indicates fragmentation of gypsum crystals along cleavage planes as the result of intense air turbulence. This is also confirmed by the simultaneous abrasion and fragmentation of tephra particles from layer 2a to 2b (Fig.9). The occurrence of strontium sulphate also as individual rounded particles attests for its sedimentary origin (Fig. 11h). Such an important aeolian input of sulphate salts is unique to the 4 kyr. B.P. event as compared to Holocene soils and earlier deposits of the studied region [5].

Observations under BSE (backscattered electron microscopy) and X-ray analysis, furthermore, reveals the occurrence of two types of glass. The first one (Fig. 11a), that is restricted to the tephra particles themselves and homogenous throughout the layer, corresponds to the volcanic glass *strict sense* as previously measured [29]. The second glass occurs as thin coatings around all sand-sized grains of layer 2a (Fig. 11a, 11c, 11e), as thin threads and domains across porous grains and aggregates (Fig. 11f, 11g, 11h) and as scattered domains in the packing porosity. Analyses with an energy dispersive X-ray spectrometer indicates major geochemical differences as compared to the typical volcanic glass (large dominance of calcium and reduced amount of potassium, abundance of Mg, lack of Na, greater abundance of iron) and significant variability of the major element composition across and between individual coatings or domains. The puzzling pattern of the Mg-Ca glass suggests that it was injected as vapour throughout the volcano-sedimentary deposit and rapidly solidified before air transportation. Theresence of Mg-Ca glass coatings around highly fissured grains (see for example Fig. 11c, 11e) suggests that the glass injection and its solidification



© Archaeopress • Provided by the NASA Astrophysics Data System

1998ncdb.conf...93C



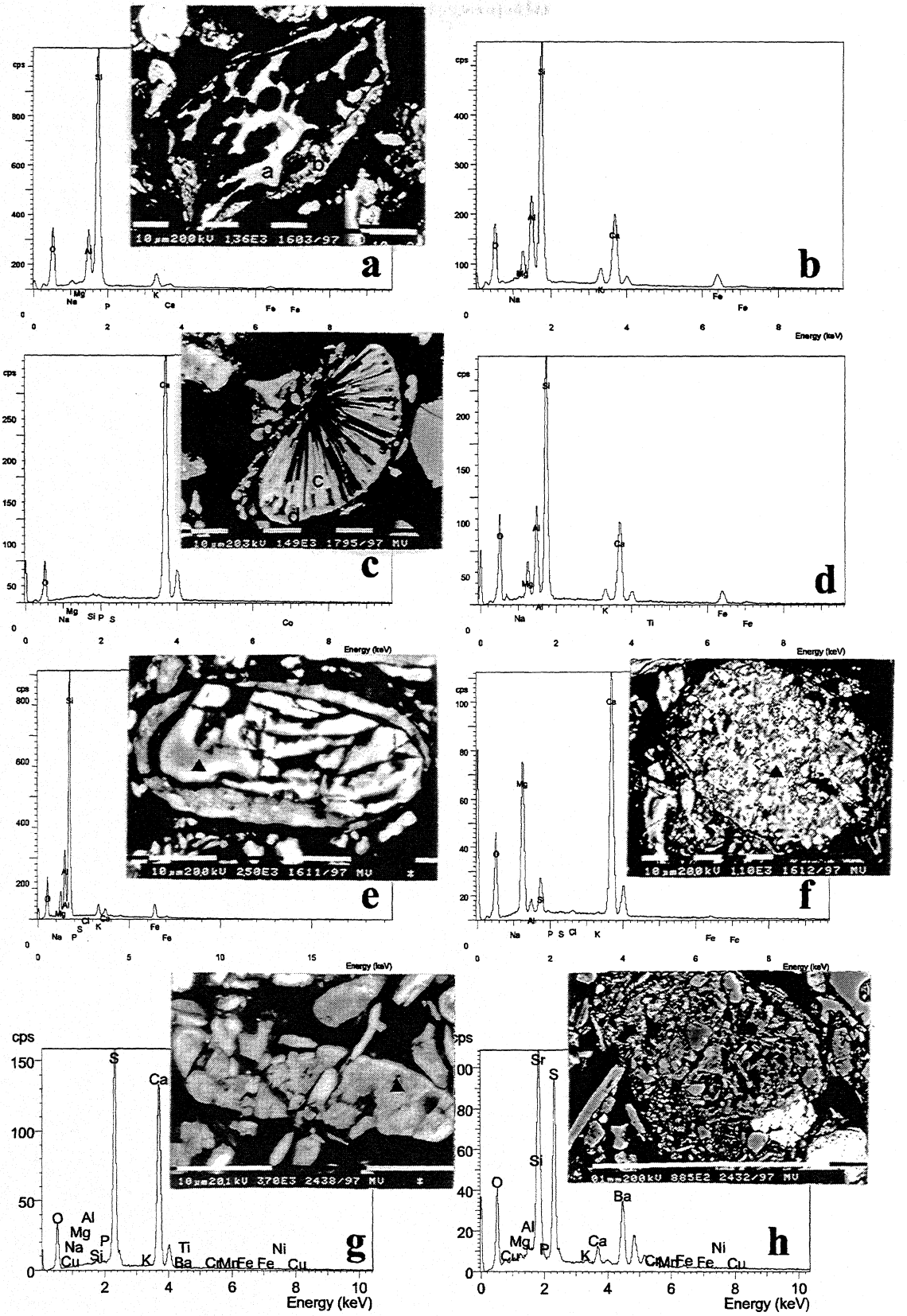


**Fig. 11**. SEM views and EDS analyses of selected particles from the tephra-rich deposit, Abu Hgeira 2. (a) EDS spectra and view of a typical tephra grain coated by Ca-Mg glass; (b) EDS spectra of Ca-Mg glass coating around the tephra grain viewed in (a); (c) sectioned fibro-radiated calcite spherule with a glass coating; (d) EDS spectra of the Ca-Mg glass around the fibro-radiated calcite spherule viewed in (c); (e) Ca-rich glass coatings around highly fragmented grains; (f) view and EDS spectra of a highly fragmented dolomite grain; (g) photo: threads of magnesio-calcic silicate glass accross a highly porous sulfate grain (EDS spectra); (h) salt inclusion (barium and strontium sulfate) within a compound, exogenous grain.

© Archaeopress • Provided by the NASA Astrophysics Data System

1998ncdb.conf...93C



occurred instantaneously after their disintegration and therefore contributed to preserve the original shape of the grains by holding the fragments together.

## 9. Discussion

The interpretation of the facies and features listed above lead us to conclude that the tephra-rich layer is, from a sedimentological view-point, a secondary volcano-sedimentary deposit that is, itself, derived from volcano-sedimentary formations. Its deposition is, therefore, not linked to a volcanic explosion but to an unusual air turbulence that induced violent reworking of the initial volcano-sedimentary formations and their transport over long distance. Lack of mixing with soil and sedimentary materials from northern Syria suggests transport as a dust plume of initial high energy that strongly resembles a volcanic one and explains our previous confusion. However, the unique petrographic composition rules out a misinterpretation with an aeolian accumulation that would derive from violent dust bowls generated from the Syrian desert by horizontal wind turbulence during exceptional droughts [5]. Consequently, the seminal air turbulence is unlikely to be linked to a climate disturbance and remains, so far, unexplained.

Evolution from layer 2a to 2b, which was originally interpreted as an abrupt increase in aeolian deflation and aridity following the tephra fall [29], is now concluded to express the inherent properties of the dust plume: firstly accumulation of the coarser debris (layer 2a) followed instantaneously by deposition of the fine dust load that would derive from pulverisation of the initial one (layer 2b). The first evidence of a regional climate disturbance is expressed by deposition of the overlying layer 3. Its sedimentary facies, typical of torrential mass flow indicates occurrence of exceptional heavy rains that contributed to seal instantaneously the tephra-rich layer, and preserve it from subsequent pedogenesis. The rapidity of the fossilisation suggests a causal linkage between production of the dust plume and the subsequent heavy rains, possibly related to a cloud condensation nuclei effect [8].

The refined investigations reported here reinforce the correlation we previously established between the thick tephra-rich deposit identified at Abu Hgeira 2 and the presence of a dust layer with an unusual petrographic assemblage [29]. The spatial stratigraphic linkage between the two facies is now reinforced by the occurrence of similar micro-debris that have never been observed in the local soils and geological formations, particularly calcite spherules, acid rocks, gabbros, dolomite and marine bioclasts. Moreover, the two stratigraphic units indicate an uncommon airborne origin as compared to the regional aeolian component and, therefore, can be considered as two distinct facies of the same event. The normal aeolian component comprises either sand-sized grains locally reworked by saltation from bare surface soils during prolonged droughts marked by he influence of unstable air masses [5] or fine silt-sized particles that are issued from atmospheric dust loading during arid phases marked by increased southerly penetration of summer northwesterly winds [31]. The latter are generally mixed with the local aeolian dust, homogenised during soil development, and therefore leaves just a small increase of the illite-kalonite clay component that can be quantified only by using subtle X-ray treatments [10].

The dust layer reported here not only forms a distinct stratigraphic unit that attests for rapid deposition, but also presents a petrographic assemblage with a clear and important exogenous component, appearing as an uncommon airborne sediment that originates from long distance transport of sand-sized particles. In the absence of an analogue for this mode of airborne transport, not only from geological records but from experiments [21], the large size of exogenous micro-debris, particularly for the tephra-rich deposit, indicates that the source materials were originally propelled at a great velocity. Furthermore, absence of a cementing agent around and within multi-minerals sand-sized particles suggests that a thin hydrated film prevented them from disintegration during transport. The reduced mixing with local soils for the tephra-rich deposit, the abundance of large sized exogenous aggregates, the well-preserved pseudo-sand facies and its significant thickness as compared to opposed characteristics for the dust layer might result from a higher water content for the former, even possibly in a frozen state as indicated by the diagnostic fabric observed.

The reverse proportion of exogenous limestones, that include both bioclasts and dolomite fragments, versus fibro-radiated calcite spherules, of the tephra-rich layer as compared to the dust layer, and their presence in the former mainly as fragments, is one of the puzzling differences between the two facies. The absence of similar spherules in the local geological deposits, soils or archaeological sediments proves that they also have an exogenous origin. However, they cannot be mistaken for marine micro-fossils as shown by their specific morphology, crystallography, size and colour, and confirmed by their too-light isotopic values for marine carbonates. They share some similar properties, except for their smaller size, with calcite spherules recognised in the Cretaceous/Tertiary Chicxulub ejecta deposits and assigned as condensation products formed by the large asteroid impact that vaporised high amount of carbonates [22]. However, the occurrence of multi-spherules accompanied by silicate cements between individual elements in the dust layer indicates that the spherules formed from an heterogeneous medium that is more likely to be a fluid than a vapour. The geochemical and morphological diversity of carbonate-rich spherules, their close association with the silica and alumino-silicated spherules, together with presence of various exogenous rock fragments, suggest that all these fragments are genetically linked. They represent a broad spectrum of ejecta reflecting both the geological complexity of the source areas, formed of sedimentary, volcanic, metamorphic and igneous rocks, and differential thermic alteration of the original rocks. The predominance of weakly altered rock fragments in the tephra-rich deposit compared to the abundance of highly altered rocks and spherules in the dust layer strengthens the hypothesis of a higher water content, possibly in the form of ice crystals, that would have partly preserved the original properties of the ejected rocks. The latter would have been transported as condensed materials, therefore explaining its deposition on a restricted area. In contrast, the extension of the dust layer and its great spatial variability would trace the propagation of a high energetic ejecta plume where both liquid and vapour phases would have coexisted, formed of rocks, sediments and soils ejected from a wider area. The resence of a hydrated form of calcium sulphate in the tephra-rich layer as opposed to the dehydrated calcium sulphate (bassanite) in the dust layer is also consistent with the hypothesis of different conditions for the two parts of the ejecta plume.

The two distinct depositional episodes identified in sites offering an expanded signal suggest a first stage consisting of deposition of the coarser fragments from the high energetic ejecta plume, later followed by settling of the finer debris and neoformed products from condensed droplets, i.e. the calcite spherules. The synchronous occurrence of wild-fires and physical disruption of surface soils and constructions during the first phase provide evidence for instantaneous ignition by fallout-induced lightning over a wide area and a low intensity small-scale explosion.

The diversity of these manifestations are inconsistent with the ones which would be induced by volcanic explosion.



© Archaeopress • Provided by the NASA Astrophysics Data System

1998ncdb.conf...93C



These might, eventually, produce physical disturbances and wild-fires but only in the close vicinity of the explosion centre and are always characterised by passive deposition of the plume ejecta after its long distance transport [24]. Interpretation of the sedimentary facies of the tephra-rich deposit has allowed us to establish the detrital origin that the potassic-rich component presents as typical tephra particles. The calco-magnesian glass component showing a wide diversity of forms, from vesicular grains to spherules, has, however, never been identified as typical tephra shards. Therefore, its presence cannot be linked with a volcanic explosion that would have produced a tephra plume.

The loosely-packed structure of the lowermost part of the tephra-rich facies (layer 2a) is interpreted as reflecting the same manifestation as the one responsible for the uncommon mechanical breakdown of the soil aggregates below the thin dust layer. The thick exploded facies observed locally in archaeological sites reflects the more important effect of the physical disruption on the high mud brick walls as compared to the flat topography of the surrounding landscapes. The synchronous incorporation of aggregates issued from natural soils suggests that the physical fragmentation was associated with violent air turbulence similar to the ones contemporaneous with deposition of the tephra-rich layer at Abu Hgeira 2. The spherule-rich upper unit in archaeological sites would represent the very last phase of the event marked by deposition of fine-textured dust just following the surficial shock, before the return to normal conditions. Specific areas of archaeological sites, thus, appear to offer an expanded signal of the event, as compared to the one recorded by natural landscapes. This has made it possible to capture a series of short phases within a time interval that might not have exceeded a few hours.

## 10. Concluding remarks

Evidence collected over a wide area of northern Syria indicates the occurrence of an explosive phenomenon at ca. 4000 B.P. (i.e. 2350 cal B.C.) that differs in many aspects from a volcanic explosion and dispersion of its volcanic ejecta plume. The explosion is hypothesised to have affected complex geological terrains consisting of sedimentary, igneous, metamorphic and volcanic rocks, closely associated with water bodies rich in various types of salts. The strong contrast observed between the two distinct facies identified for this event is concluded to reflect heterogeneity of the ejecta produced from the source areas, both in term of water content and energy of the initial pulverisation.

Although the source of the ejected materials remain to be identified, petrography of the micro-debris ejected refutes an origin from northern Syria. The evidence presented here for a wide distribution of the benchmark dust layer should motivate extension of research to the entire Middle-East, the Mediterranean basin and even to regions further afield to define in a complete fashion the conditions of the ejecta dispersion, the synchronous phenomena, particularly the wild-fires and the surface shock, and the location of the explosion. This process should also greatly benefit from further detailed geochemical investigations of the unique dust spike identified at the same period in other regions, particularly the Gulf of Oman and Lake Van and suspected to relate to the same event [16, 28].

Moreover, our data suggest the need to revise certain concepts of palaeoclimatology that widely accept a straightforward causative linkage between a dust spike and an abrupt aridification. Our own previous misinterpretation of an unusual air turbulence as a climate induced wind intensification illustrates the difficulty in avoiding such a confusion. The related mechanisms appear to be rather similar but involve different time intervals: a few seconds for the first; and a few decades for the aridity signal. Such a high time resolution is certainly difficult to obtain in most sedimentary records, particularly in calm water bodies that might blur a very short signal into an annual dust input. Furthermore, this type of depositional environment is expected to attenuate synchronous physical disturbances that are, however, of major importance in defining exactly the conditions of dust deposition. The great diversity of the records reported here illustrate completeness of information provided by various terrestrial contexts that specifically reacted to an exceptional situation. The record from archaeological sites, when disentangled from possible confusion with human actions, offers the advantage of presenting locally an expanded signal, ideal in tackling the succession of very short episodes.

The refined investigations reported here fully-confirm the abruptness of the event, the exact date of which is, unfortunately, obscured by constraints inherent in the calibration programmes of $C^{14}$ radiometric ages. The blind test successfully performed on the three archaeological sites that gave exactly the same chronological position, i.e. at the transition between the Early Dynastic period and the early Akkadian one, shows the great potential of this event to be used as a reliable stratigraphic marker competitive with historical documents. Refined examination of archaeological data, particularly at regional and inter-regional levels, should also help to determine the consequential effects of this unique event on social behaviour. The revised dating and interpretation reported here cancel our previous evidence that supported the causative linkage between this event, an abrupt climate change and collapse of the Akkadian Empire. Documenting the consequences of such a massive and instantaneous atmospheric dust load on the regional and global climate is beyond the scope of this paper. The evidence we provided for exceptional heavy rains suggests significant short-term effects consistent with climate perturbation known to be induced by massive smoke and dust injection [25].

Although our data refute the synchronous occurrence of a volcanic explosion and provide an alternative explanation for the coexistence of a thick tephra accumulation and micro-debris from volcanic rocks, importance of the spherule component in the ejecta produced remains a puzzling question. Abundantly reported from past geological records, the presence of spherule-rich layers as possible diagnostic markers of extra-terrestrial impact has been fiercely debated, but it appears they are often associated with volcanic events [15, 17, 26]. Therefore, unambiguous evidence, such as shocked quartz, the presence of tektites, an iridium anomaly, or the occurrence of silicon carbide and diamond are generally preferred to recognise impact-induced ejecta layers [14]. None of these fingerprints has so far been retrieved from the 4 kyr. B.P. dust layer. However, the occurrence of multi-site ignition together with black carbon production resulting from extensive biomass burning, also reported to be caused by asteroid impacts [32], provides indirect evidence to support an extra-terrestrial hypothesis. Various puzzling particles of the dust assemblage still require to be further elucidated, i.e. the carbon-rich black vesicular grains and the metal grains possibly linked to impact-induced lightning [9], and also the nature of the phenomenon responsible for the propagation of a surface shock wave and local explosion.

## Acknowledgements

Our sincere gratitude for continuing support goes especially to the Syrian Directorate-General of Antiquities and Museums, Damascus, Professor Dr Sultan Muhesen. We are very grateful to A. Suleiman for providing field assistance at Abu Hgeira. We thank J. Oates, A. Pruss and H. Weiss for their authorisation respectively at

© Archaeopress • Provided by the NASA Astrophysics Data System

1998ncdb.conf...93C



Tell Brak, Tell Chuera, Tell Leilan and surrounding sites during excavations under their supervision. We thank H. Cachier and S. Ruellan at the LSCE, Gif-sur-Yvette, France for black carbon analyses, M. Chaussidon and C. France-Lanord at CRPG, Nancy, France for stable isotope analyses, M. Hardy at INRA, Orléans, France, for X-ray clay analysis, N. Fedoroff at INA P-G, Grignon, France, for assistance with Soil Micromorphology, A.-M. Jaunet and M. Pernes at CNRA, Versailles, France for SEM and X-ray technical assistance, R. Rocchia at the LSCE, Gif-sur-Yvette, France, for Neutron Activation analyses and N. Tisnerat at the LSCE, Gif-sur-Yvette, France, for AMS $C^{14}$ measurement.

## References


1. Aid-Boudjera, M. (1995) *Archivage des combustions du passé dans les sédiments marins et continentaux*. D.E.A. Université Pierre et Marie Curie, Paris.
2. Cachier, H. and Ducret, J. (1991) Influence of biomass burning on equatorial African rains. *Nature* **352**, 228-230.
3. Cammas, C., Wattez, J. et Courty, M.A. (1996) L'enregistrement sédimentaire des modes d'occupation de l'espace, *The colloquium of the XIII International Congress of Prehistoric and Protohistoric Sciences. 3- Paleoecology*, (L. Castelletti and M. Cremaschi, eds.). A.B.A.C.O. edizioni, Forli, Italie, 81-86.
4. Cleuziou, S. (1994) La chute de l'empire d'Akkadé: hommes et milieux au Moyen-Orient. *Les Nouvelles de l'Archéologie* **56**, 45-58.
5. Courty M.A. (1994) Le cadre paléogéographique des occupations humaines dans le bassin du Haut Khabour (Syrie du nord-est). Premiers résultats. *Paléorient* **20(1)**, 21-59, CNRS (ed.), Paris.
6. Courty, M.A., Cachier, H., Hardy, M. and Ruellan, S. (1998) Soil record of exceptional wild-fires linked to climatic anomalies (inter-tropical and Mediterranean regions). *Actes du XVIeme Congrès Mondial de Science du Sol, Montpellier 1998*.
7. Courty M.A., Goldberg P. and Macphail R.I. (1989) *Soils and micromorphology in archaeology*. Cambridge Manuals in Archaeology. Cambridge University Press.
8. Courty, M.-A. and Weiss, H. (1997) The scenario of environmental degradation in the Tell Leilan region (N.E. Syria) during the late third millennium abrupt climate change, in NATO ASI Series, Vol. I. 49, *Third Millennium BC abrupt Climate Change and Old World Collapse*, N. Dalfes, G. Kukla and H. Weiss (eds). Springer-Verlag. Berlin. Heidelberg, 107-148.
9. Essene, E.J. and Fisher, D.C. (1986) Lightning strike fusion: extreme reduction and metal-silicate liquid immiscibility, *Science* **234**, 189-193.
10. Gaffie S., Bruand A. and Courty, M.A. (1997) A multilevel approach of structuration in time of soil systems in north-eastern Syria. *International Symposium on Soil System Behaviour in Time and Space, Vienna 1997*. Austrian Soil Science Society, Vienna. 145-148.
11. Gasse F. and Van Campo E. (1994) Abrupt post-glacial events in West Asia and North Africa monsoon domains, *Earth Planet. Sci. Lett.* **126**, 435-456.
12. Glassner J.-J. (1994) La chute de l'empire d'Akkadé, les volcans d'Anatolie et la désertification de la vallée du Habur, *Les Nouvelles de l'Archéologie* **56**, 49-51.
13. Kerr, R.A. (1998) Sea-floor dust shows drought felled Akkadian Empire, *Science* **279**, 325-326.
14. Koeberl, C. (1994) Tektite origin by hypervelocity asteroidal or cometary impact: target rocks, source craters, and mechanisms, *Geological Society of America, Special Paper* **293**, 133-151.
15. Koeberl, C. and Reimold, W.U. (1995) Early Archaean spherule beds in the Barbeton Mountain Land, South Africa: no evidence for impact origin, *Precambrian Research 7, 1*, 1-33
16. Lemcke, G. and Sturm, M. (1997) $\delta^{18}O$ and trace element measurements as proxy for the reconstruction of climate changes at Lake Van (Turkey): preliminary results, in: NATO ASI Series, Vol. I. 49, *Third Millennium BC abrupt Climate Change and Old World Collapse*, N. Dalfes, G. Kukla and H. Weiss (eds). Springer-Verlag. Berlin, Heidelberg, 653-678.
17. Melosh and Vickery, M. (1991) Melt droplet formation in energetic impact events, *Nature* **350**, 494-497.
18. Oates, J. (1994) Excavation at Tell Brak, *Iraq* **56**, 174-175.
19. Orthmann, W., Pruss, A. and Der Palast, F. (1995) Ausgrabungen in Tell Chuera, *Nordost-Syrian I*, 127-172, Saarbruecken
20. Panomarev B.Y. and Bishev A.S (1966) *The geological map of Syria*, V.P. Ponikarov (ed.). Sheets J-37-V, XI. Syrian Arab Republic. Ministry of Industry. Department of Geological and Mineralogical Research.
21. Pettijohn, F.J., Potter, P.E. and Siever, R. (1987) *Sand and Sandstone*, Springer-Verlag New York.
22. Pope, K., Ocampo A.C., Fisher, A.G., Morrison, J. and Sharp, Z. (1996) Carbonate condensates in the Chicxulub ejecta deposits from Belize. *Proceedings of the XXVII Lunar and Planetary Science Meeting*, 1045-1046.
23. Ruellan, S. (1996) *Archivage sédimentaire et glaciaire du carbone particulaire*. D.E.A. Université Pierre et Marie Curie, Paris.
24. Sigurdsson, H. (1990) Evidence of volcanic loading of the atmosphere and climatic response, *Palaeogeography, Palaeoclimatology Palaeoecology* **89**, 277-289.
25. Toon, O.B., Pollack, J.B., Ackerman, T.P., Turco, R.P., McKay, C.P. and Liu, M.S. (1982) Evolution of an impact-generated dust cloud and its effects on the atmosphere, *Geological Society of America Special paper* **190**, 187-200.
26. Wei, W. (1995) How many impact-generated micro spherule layers in the upper Eocene? *Palaeogeography, Palaeoclimatology, Palaeoecology* **114**, 101-110.
27. Weiss, H. (1990) Tell Leilan 1989: New data for Mid-Third Millennium Urbanization and State formation, *Mitteilungen der Deutschen Orient-Gesellschaft*, **122**, 193-218. Berlin, Sonderdruck Aus.
28. Weiss, H. (1997) Late third millennium abrupt climate change and social collapse in West Asia and Egypt, in: NATO ASI Series, Vol. I. *49 Third Millennium BC abrupt climate change and old world collapse*, N. Dalfes, G. Kukla and H. Weiss (eds). Springer-Verlag. Berlin. Heidelberg, 711-723.
29. Weiss, H., Courty, M.A., Wetterstrom, W., Meadow, R., Guichard, F., Senior, L. and Curnow, A. (1993) The origin and collapse of Third Millennium North Mesopotamian Civilisation, *Science* **261**, 995-1004.
30. Wilkinson T.J. (1994) The structure and dynamics of dry-farming states in Upper Mesopotamia. *Current Anthropology* **35(5)**, 483-505.
31. Wilkinson, T. (1998) Akkadian Empire: where to look? *Science* **279**, 1283-1284.
32. Wolbach, W.S., Gilmour, I., Anders, E., Orth, C.J. and Brooks, R. (1988) Global fire at the Cretaceous-Tertiary boundary, *Nature* **334**, 665-669.


© Archaeopress • Provided by the NASA Astrophysics Data System